

SUPPLEMENTAL DATA

Crystal structures and small-angle X-ray scattering analysis of UDP-galactopyranose mutase from the pathogenic fungus *Aspergillus fumigatus*

Richa Dhatwalia¹, Harkewal Singh¹, Michelle Oppenheimer², Dale B. Karr¹, Jay C. Nix³,
Pablo Sobrado², and John J. Tanner^{1,4}

From the Departments of ¹Chemistry and ⁴Biochemistry, University of Missouri-Columbia, Columbia, MO 65211, the ²Department of Biochemistry, Virginia Tech, Blacksburg, VA 24061, USA, and the ³Molecular Biology Consortium, Lawrence Berkeley National Laboratory, Berkeley, CA 94720, USA.

Running title: Crystal structures and SAXS of UGM

Address correspondence to: John J. Tanner, Department of Chemistry, University of Missouri-Columbia, Columbia, MO 65211, USA. Phone: 573-884-1280. Fax: 573-882-2754. E-mail: tannerjj@missouri.edu.

Table of Contents

Crystallization methods	S-2
Table S1. Steady state kinetics of AfUGM and K344A/K345A	S-3
Fig. S1. Electron density maps for the histidine loop in the sulfate complex and AfUGM _r .	S-4
Fig. S2. UDP-Galp recognition by eukaryotic and bacterial UGMs.	S-5
Fig. S3. Comparison of AfUGM and protoporphyrinogen oxidase.	S-6
Fig. S4. Proposed chemical mechanism.	S-7

Crystallization—Crystallization screens of AfUGM and Se-Met AfUGM were performed at 21°C and 4°C using the sitting-drop and hanging-drop methods of vapor diffusion, as well as microbatch. These screens were performed using ligand-free protein and protein that had been incubated with UDP-glucose, UMP, or UDP.

Initial structure determination efforts were hampered by translational pseudosymmetry (TPS). Crystal screening and optimization yielded two crystal forms that exhibit TPS. One of these forms appeared as hexagonal blocks in ammonium sulfate and diffracted to 3.4 Å resolution. The optimal reservoir contained 1.6 M ammonium sulfate, 5 % PEG 400, and HEPES buffer at pH 7.5. The apparent Laue symmetry is $6/mmm$ with unit cell lengths of $a = 202$ Å, $c = 355$ Å. The native Patterson map calculated using phenix.xtriage (15) exhibited a peak at ($u = 0, v = 0, w = 0.49$) with a height of 48 % relative to the origin peak, which suggests strong TPS. This crystal form was also obtained under low ionic strength conditions, such as 13% polyethylene glycol (PEG) 8000 and HEPES buffer at pH 8.0. Curiously, the external morphology of the PEG form was thin blades instead of hexagonal blocks. Nevertheless, the lattice and TPS were identical to that of the ammonium sulfate form. Various PEG solutions also yielded an orthorhombic crystal form, which diffracted to 3.2 Å. The apparent Laue symmetry is mmm with $a = 111$ Å, $b = 207$ Å, and $c = 234$ Å. The native Patterson map exhibited a strong (22 - 45 %) off-origin peak near (0, 0.25, 0.5), indicating TPS. Se-Met SAD phasing was

attempted with these crystal forms, but the maps were not interpretable.

Additive screening was used to identify new crystal forms. The most promising result was obtained using ammonium sulfate as the precipitant and isopropanol as the additive. The inclusion of 5 % isopropanol changed the morphology from hexagonal block to hexagonal bipyramid. The apparent Laue symmetry is $6/mmm$ with cell dimensions of $a = 217$ Å, $c = 325$ Å. Note that these dimensions are about 8 % different from those obtained in the absence of isopropanol. Moreover, the native Patterson map did not indicate TPS. However, these crystals diffracted to only about 5.5 Å resolution. Structure determination via Se-Met SAD phasing failed, due presumably to poor data quality.

Several site-directed mutants of AfUGM were screened to identify crystal forms that are free of pathologies and diffract to higher resolution. The mutations were designed from a homology model of AfUGM calculated using Phyre (16). The mutant enzymes that were subjected to crystal screening included the predicted active site mutants W167A, R211A, R327K, and W204A, as well as the predicted surface double mutants K231A/K233A, K239A/K241A, K344A/K345A, and K363A/E364A. Most of the aforementioned undesirable crystal forms were also observed with the mutant enzymes. However, a new hexagonal crystal form was discovered with K344A/K345A, and this crystal form was used for structure determination as described in the main text.

TABLE S1
Steady state kinetics of AfUGM and K344A/345A

	k_{cat}, s^{-1}	$K_M, \mu M$	$k_{cat}/K_M, \mu M^{-1} s^{-1}$
Native	60 ± 3	70 ± 10	0.84 ± 0.13
K344A/K345A	55 ± 2	70 ± 9	0.75 ± 0.07

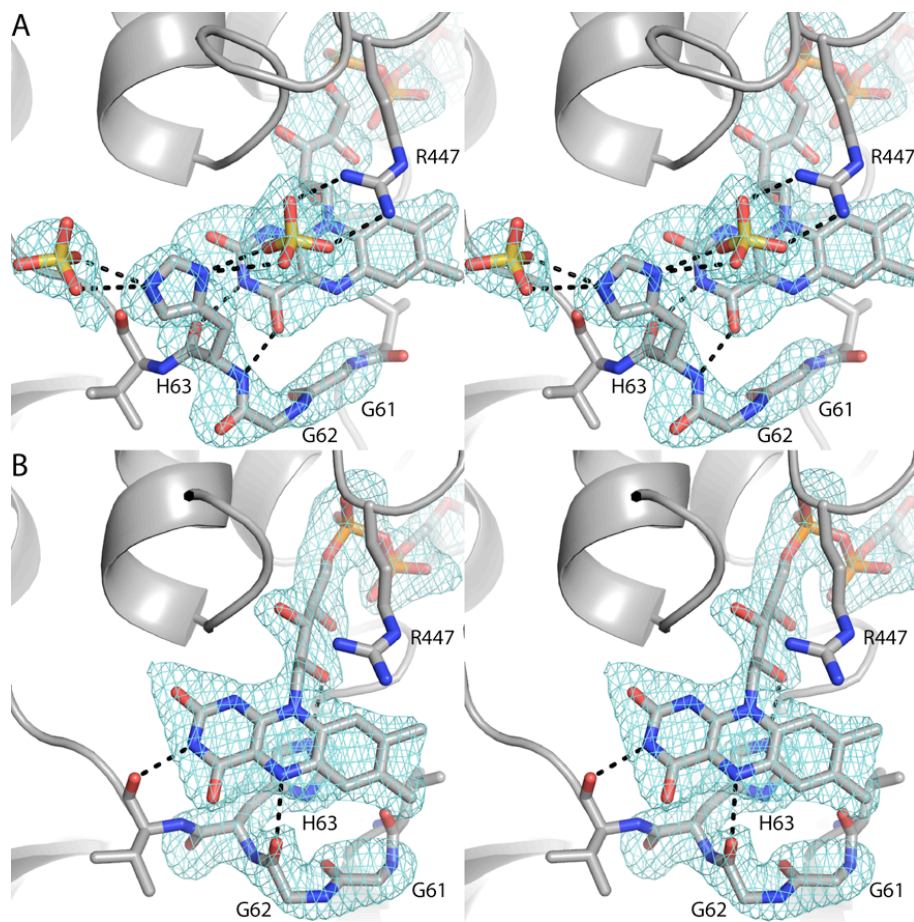


Fig. S1. Stereographic views of histidine loop in the (A) sulfate complex and (B) AfUGM_r. In both panels, the cage represents a simulated annealing σ_A -weighted $F_o - F_c$ omit map contoured at 3.0σ .

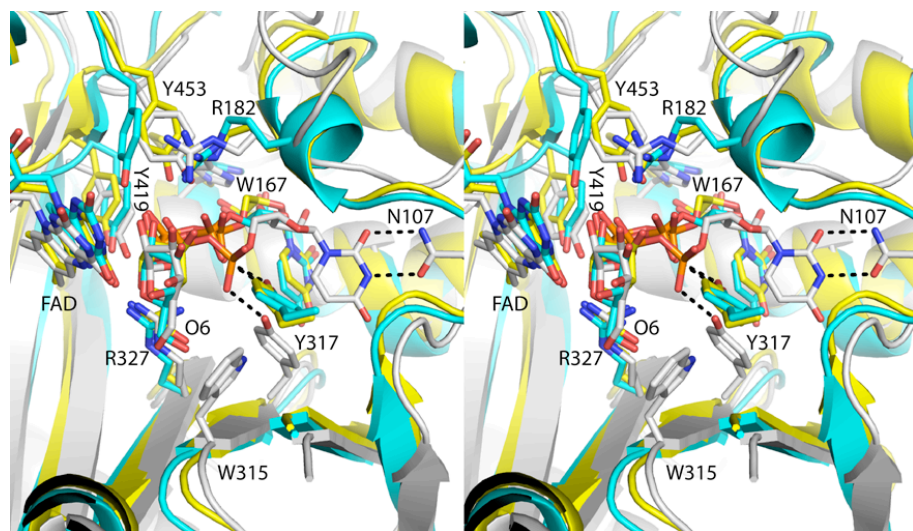


Fig. S2. UDP-Galp recognition by eukaryotic and bacterial UGMs (stereographic view). The structures of AfUGM (white), KpUGM (cyan, 3INT), and DrUGM (yellow, 3HDY) complexed with UDP-Galp are shown. Selected residues of AfUGM are noted.

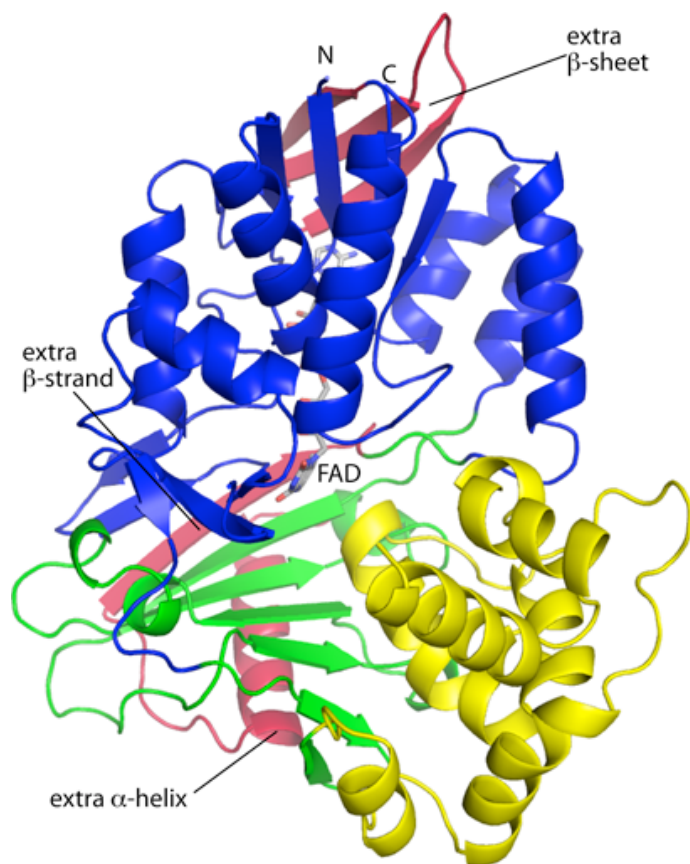


Fig. S3. Protoporphyrinogen oxidase from *Myxococcus xanthus* (PDB code 2IVD). The FAD-binding (blue), membrane-binding (yellow), and substrate-binding (green) domains correspond to UGM domains 1, 2, and 3, respectively. Red indicates elements that are common to AfUGM and PPOX but not found in bacterial UGMs.

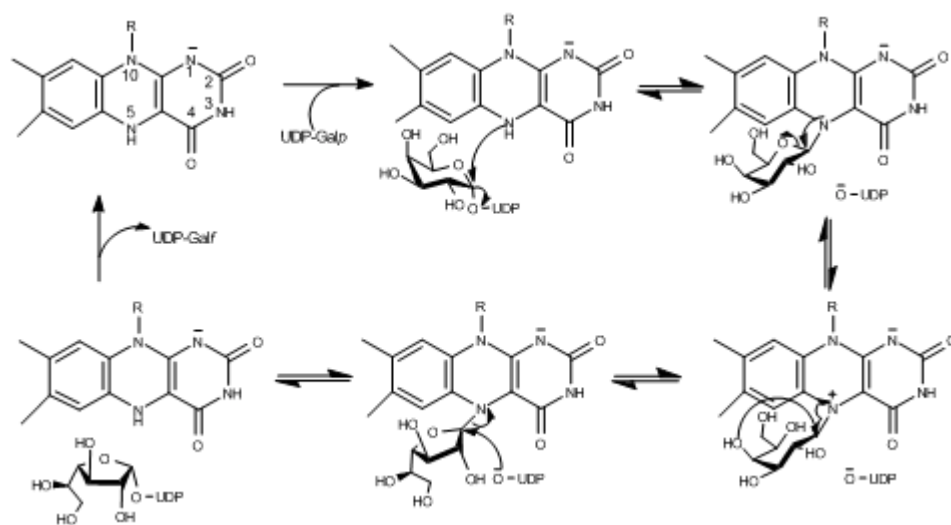


Fig. S4. Proposed chemical mechanism in which the FAD acts as a nucleophile forming an iminium ion prior to the interconversion between pyranose and furanose forms.